The EMBO Journal (2004) 23, 749–759 | © 2004 European Molecular Biology Organization | All Rights Reserved 0261-4189/04
www.embojournal.org

THE EMBO JOURNAL

Sra-1 and Nap1 link Rac to actin assembly driving lamellipodia formation

Anika Steffen[1], Klemens Rottner[1], Julia Ehinger[1], Metello Innocenti[2], Giorgio Scita[2], Jürgen Wehland[1] and Theresia EB Stradal[1,*]

[1]German Research Centre for Biotechnology, Department of Cell Biology, Braunschweig, Germany and [2]European Institute of Oncology, Department of Experimental Oncology, Milano, Italy

The Rho-GTPase Rac1 stimulates actin remodelling at the cell periphery by relaying signals to Scar/WAVE proteins leading to activation of Arp2/3-mediated actin polymerization. Scar/WAVE proteins do not interact with Rac1 directly, but instead assemble into multiprotein complexes, which was shown to regulate their activity *in vitro*. However, little information is available on how these complexes function *in vivo*. Here we show that the specifically Rac1-associated protein-1 (Sra-1) and Nck-associated protein 1 (Nap1) interact with WAVE2 and Abi-1 (e3B1) in resting cells or upon Rac activation. Consistently, Sra-1, Nap1, WAVE2 and Abi-1 translocated to the tips of membrane protrusions after microinjection of constitutively active Rac. Moreover, removal of Sra-1 or Nap1 by RNA interference abrogated the formation of Rac-dependent lamellipodia induced by growth factor stimulation or aluminium fluoride treatment. Finally, microinjection of an activated Rac failed to restore lamellipodia protrusion in cells lacking either protein. Thus, Sra-1 and Nap1 are constitutive and essential components of a WAVE2- and Abi-1-containing complex linking Rac to site-directed actin assembly.

The EMBO Journal (2004) **23,** 749–759. doi:10.1038/sj.emboj.7600084; Published online 5 February 2004
Subject Categories: cell & tissue architecture; signal transduction
Keywords: Abi; lamellipodium; Rac; WAVE

Introduction

Dynamic reorganization of the actin cytoskeleton is essential for cell migration during wound healing, embryonic development and metastasis, and is involved in bacterial and viral pathogenesis. While pathogens usurp the cellular machinery of actin polymerization in a constitutive manner, cellular responses to external signals underlie a tight spatiotemporal control. The formation of cellular projections like lamellipodia and ruffles is accompanied by rapid, site-directed *de novo* nucleation and polymerization of actin into filaments. This process is catalysed by actin nucleating factors, the most prominent of which is the Arp2/3 complex. Catalytic activation of the Arp2/3 complex is, however, mediated by the WASP/Scar family of proteins, which in turn translates extracellular signals via the small GTPases of the Rho family into actin polymerization.

It is well established that GTP-loaded Rac1 induces actin-based plasma membrane projections such as lamellipodia and membrane ruffles by activating the Arp2/3 complex via WAVE proteins (Miki *et al*, 1998; Ridley, 2001). In accordance, WAVE proteins have been found to accumulate at the tips of these projections (Hahne *et al*, 2001; Nozumi *et al*, 2003), where actin polymerization is thought to be initiated and maintained, providing the propulsive force for membrane extension. A number of additional proteins, including the signalling adaptors Abi-1 (e3b1) and Abi-2 (Stradal *et al*, 2001) as well as IRSp53 (Nakagawa *et al*, 2003), have been shown to localize, similarly to WAVE proteins, to these sites, suggesting that a multiprotein complex at lamellipodia tips may be responsible for the formation of these structures. A direct involvement of Abi and WAVE proteins in actin remodelling at membrane protrusions was further demonstrated by the observations that sequestration of Abi-1 by microinjection of polyclonal antibodies into cells (Scita *et al*, 1999) and the overexpression of the Scar/WAVE-WA domain (Machesky and Insall, 1998)—acting in a dominant-negative fashion—abolished the ability to form membrane ruffles induced by growth factor stimulation. Moreover, cells derived from WAVE2 null mice confirmed the critical role of this isoform in Rac-mediated actin-based processes (Yamazaki *et al*, 2003; Yan *et al*, 2003). Together, these data point towards a direct involvement of both protein families, Abi and WAVE, in the formation of cellular protrusions. However, it is not clear how WAVE activity is regulated at the molecular level.

Abi proteins can directly interact with a protein termed Nap1 (Nck-associated protein) (Yamamoto *et al*, 2001), which was shown before to be linked to Rac1 via p140 (Kitamura *et al*, 1997). The latter protein corresponds to Sra-1 capable of direct interaction with both Rac1 and Nap1 (Kobayashi *et al*, 1998). A more recent study reported the isolation of protein complexes from bovine brain containing most of the molecules mentioned above, including Nap1, the Sra-1 homologue PIR121, WAVE1 and Abi proteins. Based on actin polymerization experiments employing the aforementioned complex, PIR121 and Nap1 were concluded to inhibit WAVE function *in vitro* (Eden *et al*, 2002). However, whether Sra-1 and Nap1 exert a stimulatory or inhibitory effect on WAVE-mediated actin assembly *in vivo* remained to be established.

Interestingly, the *Drosophila* homologue of Nap1, KETTE, has been implicated in the migration of Glia cells in the developing embryo and an altered actin cytoskeleton was observed in various cell types in mutant *kette* embryos (Hummel *et al*, 2000). Additionally, the *Caenorhabditis elegans* homologues of both Sra-1 and Nap1 known as

*Corresponding author. German Research Centre for Biotechnology (GBF), Department of Cell Biology, Mascheroder Weg 1, D-38124 Braunschweig, Germany. Tel.: +49 531 6181 442; Fax: +49 531 6181 444; E-mail: ths@gbf.de

Received: 15 September 2003; accepted: 18 December 2003; Published online: 5 February 2004

GEX-2 and GEX-3, respectively, were found to be essential for hypodermal cell migration during embryonic development and the phenotypes described for loss of function of both gene products were virtually identical (Soto *et al*, 2002).

Here we show that mammalian Nap1 and Sra-1 are an integral part of a WAVE2/Abi-1-containing lamellipodial complex, which is dynamically relocalized to membrane protrusions induced by activated Rac. Furthermore, we provide evidence that loss of function of either protein, Sra-1 or Nap1, completely abolishes the ability of cells to respond to Rac activation with actin-based membrane protrusion. Thus, both proteins are essential components of a lamellipodial complex, controlling Rac-dependent actin remodelling at these sites.

Results

Sra-1 and Nap1 localize to lamellipodial protrusions

Nap1 was described as a potential interaction partner of Abi-1 (Yamamoto *et al*, 2001) and Sra-1 was found to bind to profilin II (Witke *et al*, 1998). Furthermore, Nap1 and Sra-1 were repeatedly shown to interact with each other (Kitamura *et al*, 1996, 1997; Kobayashi *et al*, 1998; Witke *et al*, 1998; Soto *et al*, 2002). As we had already described that Abi-1 (Stradal *et al*, 2001) and profilin II (Geese *et al*, 2000) can target to the tips of lamellipodial protrusions, we asked whether this may also be true for Nap1 and Sra-1. In order to examine the subcellular localization of Sra-1 and Nap1 in motile cells, we generated polyclonal antibodies specific for these proteins (see Supplementary Figure 1) and double-stained B16-F1 cells that were stimulated with aluminium fluoride (AlF), demonstrated earlier to enhance extensively lamellipodia formation in these cells (Hahne *et al*, 2001), for the respective component and for the actin cytoskeleton. Interestingly, both proteins (Figure 1A and B) were highly enriched at the tips of lamellipodia in front of the bulk of lamellipodial actin filaments (Figure 1A′ and B′), but were absent from other cytoskeletal structures, highly reminiscent of the subcellular positioning of Abi and WAVE proteins (Stradal *et al*, 2001; Nozumi *et al*, 2003). The same type of localization was observed in fibroblasts (Figure 1C–D′).

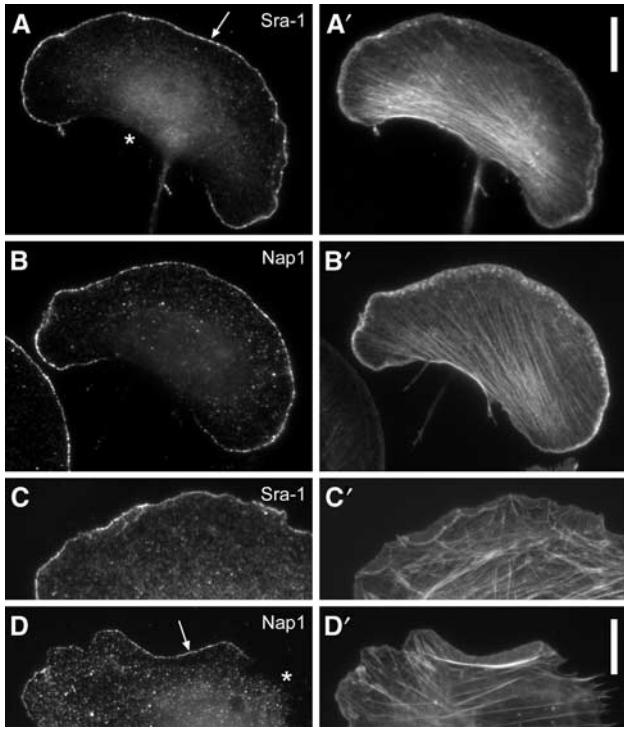

Figure 1 Sra-1 and Nap1 localize at the tips of lamellipodial protrusions. B16-F1 melanoma cells (**A**–**B**′) and Swiss 3T3 fibroblasts (**C**–**D**′) were immunolabelled for Sra-1 (A, C) or Nap1 (B, D) and counterstained for the actin cytoskeleton with fluorescent phalloidin (A′, B′, C′, D′). Note the localization of both proteins at the very edge (arrows in A, D) of protruding lamellipodia, but the complete absence of these proteins from zones of retraction (asterisk in D) or at the cell rear (asterisk in A). Scale bars in A′ (valid for A–B′) and D′ (valid for C–D′) represent 10 μm.

Sra-1 and Nap1 interact with Abi-1 and WAVE2

Given that Nap1 was described as a potential binding partner of Abi-1, we asked whether their colocalization might be reflected by an *in vivo* interaction, and to what extent this interaction might include Sra-1 and other components of a putative lamellipodial tip complex. To answer this question, we performed co-immunoprecipitation experiments with antibodies to both Sra-1 and Nap1 using B16-F1 cells. Sra-1 and Nap1 co-precipitated with each other, and also readily with Abi1-1 and WAVE2 (Figure 2A). Identical results were obtained when lamellipodia formation was induced by AlF treatment in B16-F1. It was demonstrated earlier that Rac can be activated by AlF treatment in neutrophils (Geijsen *et al*, 1999).

To confirm that this treatment also activates Rac in B16-F1 cells, we used the p21 binding domain (PBD) of p21-activated kinase (PAK), which binds specifically to activated GTP-bound Rac and Cdc42 (Benard and Bokoch, 2002). Immobilized PAK–PBD precipitated significantly more active Rac from lysates of AlF-treated cells than from untreated cells (Figure 2B). Hence, AlF can lead to the activation of Rac in B16-F1 cells, explaining the strong induction of lamellipodia in this system.

The efficiency of lamellipodia induction by AlF treatment of B16-F1 cells is at maximum by 15 min (Hahne *et al*, 2001). To test whether the co-immunoprecipitated Sra-1/Nap1/Abi-1/WAVE2 complex remains fully assembled at earlier time points, for example, immediately after initiation of Rac activation, we performed immunoprecipitation experiments at different time points after AlF stimulation. At no time point could we detect a dissociation of WAVE2 from or diminished binding to Sra-1 (Figure 2C), indicating that the complex is constitutively assembled in the presence and absence of active Rac *in vivo*.

To further test for the stability of the complex upon Rac activation, we sought to detect both Rac1 and WAVE2 in anti-Sra-1 immunoprecipitates, suggestive of simultaneous interactions of Sra-1 with Rac and the WAVE2-containing complex. Indeed, anti-Sra-1 immunoprecipitates not only contained Nap1, Abi-1 and WAVE2 but also ectopically expressed myc-tagged L61Rac1 (Figure 2D), showing that the presence of active GTP–Rac1 in Sra-1 immunoprecipitates does not lead to the dissociation of constituents of this complex such as WAVE2 from Sra-1. In a complementary experiment, cellular lysates were challenged with constitutively active

glutathione *S*-transferase (GST)–L61Rac1 immobilized on glutathione–sepharose. The precipitates obtained were probed for the presence of Sra-1, Nap1, Abi-1 and WAVE2. In fact, we could readily detect all these components, further supporting our finding that WAVE2 does not dissociate from Sra-1 and Nap1 even in the presence of excess amounts of GTP-loaded Rac (Figure 2E). Thus, we conclude that the Sra-1/Nap1/Abi-1/WAVE2 complex remains intact after Rac activation *in vivo*, which is in contrast to observations obtained for WAVE1 *in vitro* (Eden *et al*, 2002).

Antisera specific for WAVE1 and 3 were used to confirm the virtual absence of these isoforms from both murine B16-F1 and human VA-13 cell lines (see below). Hence, the WAVE protein detected with the pan-WAVE antiserum used was concluded to represent WAVE2 in all instances (see Supplementary Figure 2).

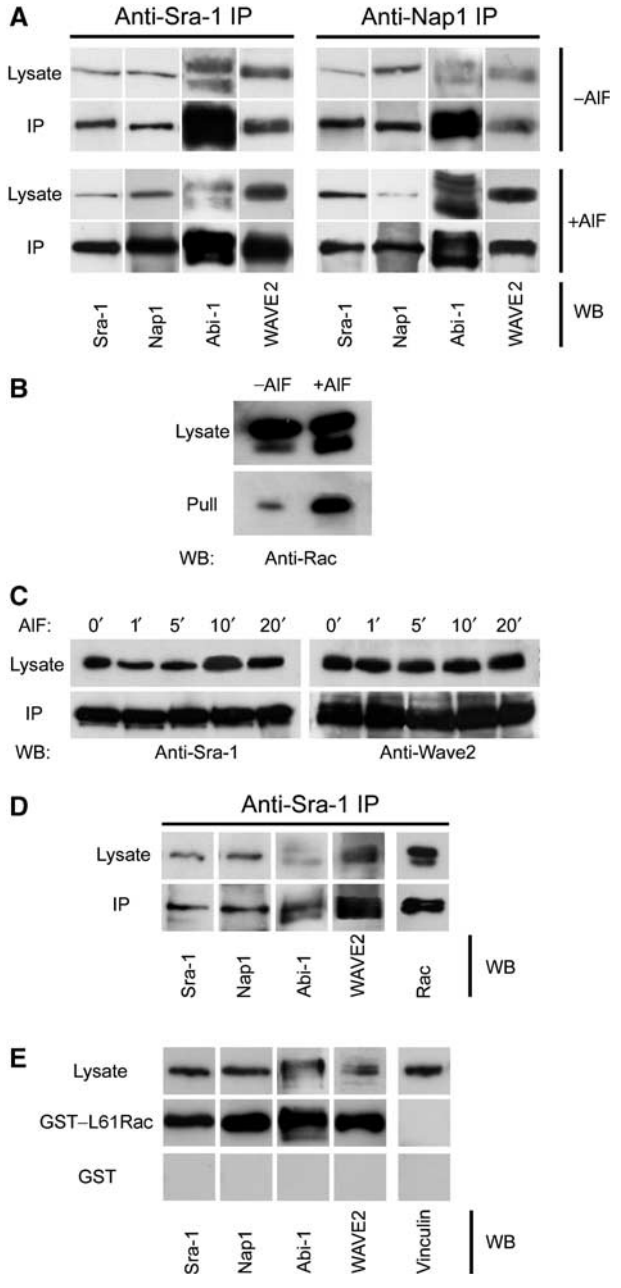

Sra-1 and Nap1 are redistributed by constitutively active Rac

Recently, actin polymerization assays with isolated complexes harbouring Nap1, PIR121, Abi-2 and WAVE1 proteins suggested an inhibitory function of Nap1 and PIR121 on WAVE-mediated actin nucleation that could be released upon interaction of this complex with activated Rac. This led to the conclusion that upon Rac binding PIR121/Sra-1 and Nap1 dissociate from WAVE proteins prior to WAVE-mediated nucleation of lamellipodial actin filaments (Eden *et al*, 2002), although this was not tested *in vivo*. To test this hypothesis, we compared the dynamics of Nap1 and Sra-1 with those of Abi-1 and WAVE2 upon microinjection of constitutively active Rac1. Microinjection of recombinant mutants of Rho-GTPases is a well-established method of characterizing their effects on actin remodelling (Ridley, 1998), and the cellular response to L61Rac1 was described in great detail (Ridley *et al*, 1992; Rottner *et al*, 1999b). Ectopically expressed Sra-1 and Nap1 fused to EGFP could readily be observed in spontaneous lamellipodial protrusions of both B16-F1 and NIH 3T3 cells (not shown) indistinguishable from the distribution of the endogenous proteins (see also Figure 1). We routinely microinjected NIH 3T3 cells that were devoid of prominent lamellipodia before injection (Figure 3A–F) and followed individual cells before and after injection in both phase contrast (Figure 3A and A′ and not shown) and fluorescent channels (Figure 3B–F′; for movies, see Supplementary information). Strikingly, Sra-1 and Nap1 were dramatically translocated to the plasma membrane and accumulated at the tips of newly forming lamellipodia immediately after microinjection (Figure 3B′ and C′). The same translocation characteristics were observed for EYFP–Abi-1 (Figure 3D and D′) and EGFP–WAVE2 (Figure 3E and E′). Microinjection of L61Rac1 into EGFP–β actin-expressing cells highlights actin rearrangements accompanying the translocation of the components described above (Figure 3F and F′). From these experiments, we conclude that Sra-1 and Nap1 display dynamics highly

Figure 2 Sra-1 and Nap1 interact with Abi-1 and WAVE2. (**A**, **B**) Sra-1 and Nap1 form a complex with Abi-1 and WAVE2. Cellular lysates and precipitates were analysed by Western blotting (WB) with the antibodies as indicated. Polyclonal antibodies raised against Sra-1 (left) as well as Nap1 (right) precipitate a multimolecular complex containing Sra-1, Nap1, Abi-1 and WAVE2, which are not dissociated by the loading of small GTPases with AlF. (A) Upper panel: Precipitates from unstimulated B16-F1 cells are indistinguishable from those (lower panel) of AlF-treated cells. Multiple bands recognized by anti Abi-1 antibodies were described to represent differential phosphorylation products (Biesova *et al*, 1997). (B) AlF treatment causes increased binding of Rac to the p21-binding domain of PAK (PAK–PBD). (**C**) Immunoprecipitations with anti-Sra-1 antibodies at different time points after AlF treatment as indicated. Lysates and precipitates were probed with anti-Sra-1 and anti-WAVE antibodies as indicated. Note the co-precipitation of WAVE2 with anti-Sra-1 antibodies at all time points after AlF treatment. (**D**, **E**) Rac associates with the intact Nap1/Sra-1/Abi-1/WAVE2 complex. (D) Cellular lysates from B16-F1 cells expressing myc-tagged L61Rac1 were subjected to anti-Sra-1 immunoprecipitation and probed for the presence of Sra-1, Nap1, Abi-1 and WAVE2 as well as for Rac1, which was readily co-precipitated with the intact complex. (E) Immobilized GST–L61Rac, but not GST alone, precipitates Sra-1, Nap1, Abi-1 and WAVE2 from B16-F1 cellular lysates, but not the focal adhesion component Vinculin assayed as negative control.

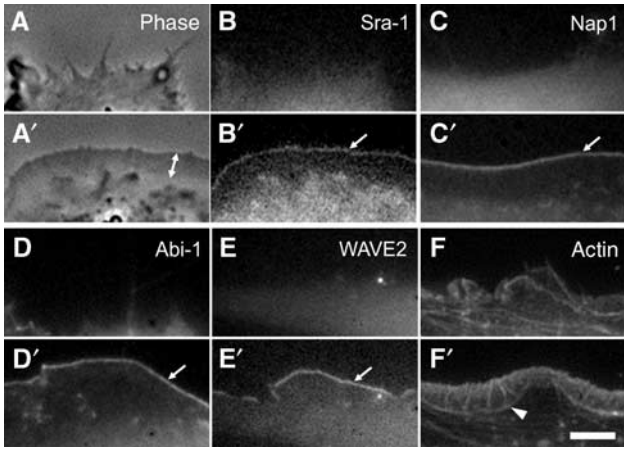

Figure 3 Sra-1 and Nap1 are redistributed by constitutively active Rac. NIH 3T3 fibroblasts expressing EGFP-tagged Sra-1 (**A**–**B**′), Nap1 (**C**, **C**′), WAVE2 (**E**, **E**′) and actin (**F**, **F**′) or EYFP-tagged Abi-1 (**D**, **D**′) were analysed by fluorescence and phase contrast video microscopy during microinjection of constitutively active L61Rac1. The panels represent video frames taken 2 min before (A–F) or 30 min after injection (A′–F′). Sra-1 (B, B′) and Nap1 (C, C′) as well as Abi-1 (D, D′) and WAVE2 (E, E′) are translocated to and concentrated at the tips of the lamellipodia induced by active Rac1 (arrows in B′, C′, D′ E′). The phase contrast panels (A, A′) of the Sra-1-expressing cell (B, B′) demonstrate the dramatic morphological change of the cell periphery upon Rac1 injection and the width of the lamellipodium (double-headed arrow in A′) as compared to recruitment of Sra-1/Nap1/Abi-1/WAVE2, which appear to be restricted to the very edge. The organization of lamellipodial microfilaments can best be appreciated with EGFP–actin (F′). The actin bundle (arrowhead in F′) marks the base of the lamellipodium. The scale bar equals 5 μm.

similar to Abi-1 and WAVE2, and that even excess amounts of GTP-bound Rac1 do not result in delocalization of Sra-1 and Nap1 from lamellipodia.

To examine the degree of translocation of Sra-1 and Nap1 to lamellipodial tips in the same cells, we cotransfected NIH 3T3 cells with EGFP–Sra-1 and Nap1 fused to monomeric dsRED (mRFP, Campbell *et al*, 2002). These cells were again subjected to Rac injection and followed in phase contrast as well as two-channel fluorescence video microscopy. Signal intensity scans across the cell periphery applied to the video data from both green and red fluorescent channels revealed that the degree of translocation by L61Rac1 of both Sra-1 and Nap1 was virtually identical (see Supplementary Figure 3 and Supplementary movie 3).

Interference with Sra-1 and Nap1 expression impairs lamellipodia formation in B16-F1 cells

Not only the localization patterns of Sra-1 and Nap1 and their dynamic translocation with Abi- and WAVE-proteins in response to Rac, but also the physical interaction of all four proteins in immunoprecipitations suggest that Sra-1 and Nap1 play a critical role in lamellipodia protrusion. However, it is not possible to delineate a stimulatory function of a given protein solely from its subcellular distribution. Hence, we decided to study the consequences of Sra-1 or Nap1 ablation by RNA interference (RNAi).

For these experiments, we employed a vector-based approach for the stable expression of short interfering RNAs (siRNA) in mammalian cells (Brummelkamp *et al*, 2002). Initially, B16-F1 cells were transfected with vectors harbouring a puromycin resistance gene and driving the expression of siRNAs directed towards transcripts of Nap1 or Sra-1 and PIR121 or with mock plasmids. Expression of the respective proteins was assessed at several time points after transfection and puromycin selection (Figure 4A). The time point of most efficient protein suppression in B16-F1 cells (Figure 4A) was chosen for the analysis of cell morphology. At day 4 after transfection, the different cell populations were stimulated to form lamellipodia with AlF, fixed, stained with phalloidin (for representative images, see Figure 4B and C), and subjected to careful morphological analysis of the cell periphery (Figure 4B′ and C′). Cells were classified according to their ability to form lamellipodia, and derived data were subjected to quantification and statistical analysis (Figure 4D). While more than 80% of mock-transfected cells ($n=590$) displayed prominent lamellipodia, the formation of these structures was reduced to 25% ($n=556$) and 11% ($n=572$) for Sra-1/PIR121 and Nap1 knockdown cells, respectively (Figure 4D).

To ensure that lamellipodia formation after Sra-1 or Nap1 ablation by RNAi is not impeded due to downregulation or inhibition of Rac1, we tested the expression of Rac1 and its ability to be activated by AlF and to interact with PAK–PBD upon siRNA treatments as compared to wild-type B16-F1 cells. Rac1 expression and increased binding to the PAK–PBD domain after AlF treatment were found to be unchanged in mock as well as Sra-1 and Nap1 siRNA-treated as compared to wild-type cells (Figure 4E).

Overexpression of WAVE2 cannot restore lamellipodia formation in Nap1 knockdown cells

In a recent exciting study, RNAi screens in *Drosophila* S2 Schneider cells revealed that ablation of dSra-1, KETTE and dAbi caused a significant reduction of SCAR/WAVE protein levels (Rogers *et al*, 2003). Interestingly, reduced WAVE expression was also observed in PIR121 null *Dictiostelium* cells (Blagg *et al*, 2003). To test whether diminution of WAVE2 can also be observed in mammalian cells after siRNA treatment targeting the components complexed with WAVE2, we probed for WAVE2 protein expression levels in control versus Nap1 knockdown cells (Figure 5A). In line with earlier reports, we could detect a significant reduction of WAVE expression upon Nap1 siRNA treatment. To test whether the reduction of WAVE expression is causative of the absence of lamellipodia, we re-expressed GFP-tagged WAVE2 in Nap1 siRNA-treated cells. However, ectopically expressed EGFP–WAVE2 was not recruited to the cell periphery and did not restore lamellipodia formation in these cells (Figure 5C).

Quantification of the number of cells lacking lamellipodia despite AlF treatment revealed no significant difference between Nap1 knockdown cells ($86.6\pm1.2\%$; $n=329$) as compared to those re-expressing EGFP–WAVE2 ($91.7\pm2.9\%$; $n=360$) (Figure 5B). Western blot analysis of parallel cell populations proved that EGFP–WAVE2 was not degraded in these experiments and that its expression was comparable to that of endogenous WAVE2 in mock RNAi-treated controls (Figure 5A). These data demonstrate that the lack of lamellipodia formation after Nap1 ablation cannot be explained by reduced WAVE2 expression levels only, but instead results from the disability of these cells to target WAVE2 to sites of actin remodelling at the cell periphery. This view is further

supported by the fact that the lack of lamellipodia in Nap1 siRNA-treated cells is accompanied by the absence not only of the remnants of endogenous WAVE2 but also of Sra-1 and Abi-1 from the cell periphery (Figure 5D–E′).

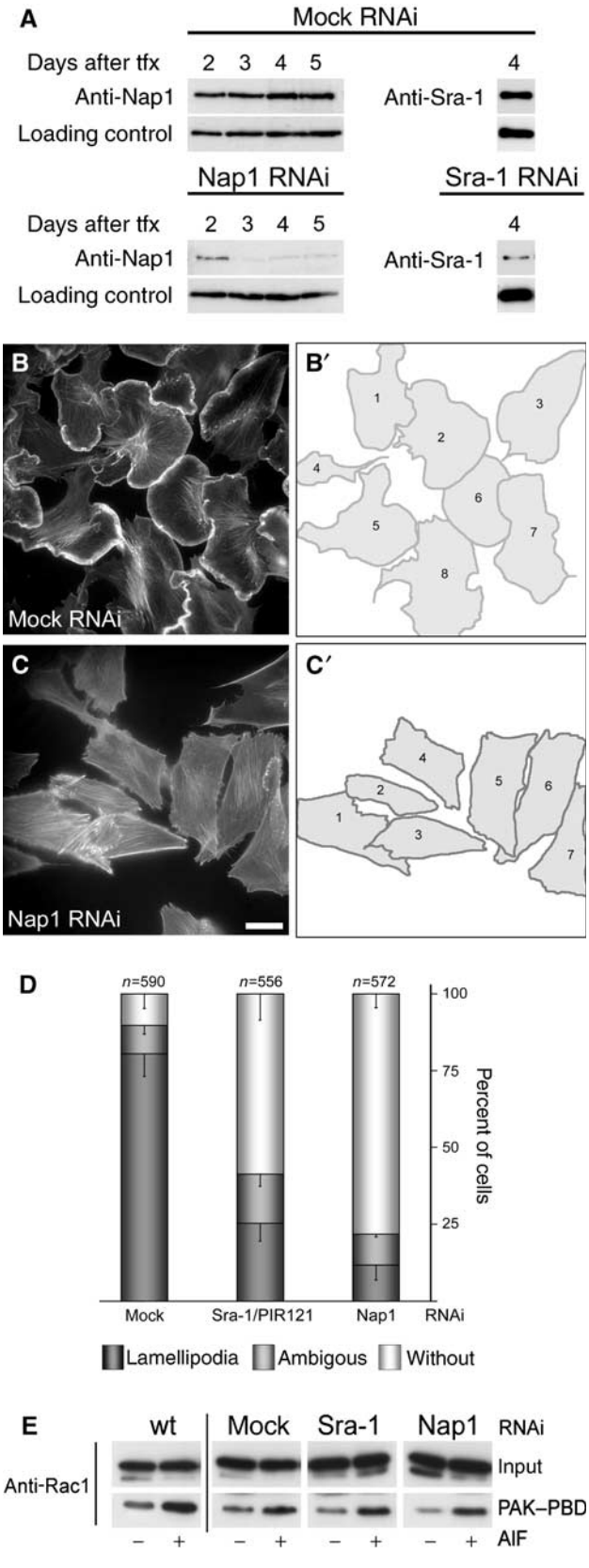

Loss of Sra-1 and Nap1 function abolishes growth factor-induced membrane ruffling in fibroblasts

The formation of Rac-dependent lamellipodia and membrane ruffles can be triggered by activation of fibroblasts with various growth factors such as epidermal (EGF) or platelet-derived growth factor (PDGF) (Hall, 1998; Ridley *et al*, 1992). To test for the role of Sra-1 and Nap1 in this response, we established RNAi-mediated knockdown of Sra-1 and Nap1 in the human fibroblast cell line VA-13. As for B16-F1 cells, the efficiency of protein suppression was assessed by Western blotting at different time points after transfection with mock versus the respective knockdown plasmids (Figure 6A). In these cells, all experiments were performed between days 5 and 7 after transfection. To test whether growth factor-induced ruffling is altered upon downregulation of Sra-1 or Nap1 expression, mock- and siRNA-treated VA-13 cells were serum starved for 30 min and stimulated with either EGF (100 ng/ml) (Figure 6B–D) or PDGF (10 ng/ml) (Figure 6E–G) for 15 min, fixed, stained with phalloidin and subjected to careful quantitative analysis. While mock-treated cells displayed prominent membrane ruffling after stimulation with both EGF (Figure 6B) and PDGF (Figure 6E), this response was severely compromised upon Sra-1 (Figure 6D and G and not shown) or Nap1 knockdown (Figure 6C and F). Quantification of this response revealed that 82% ($n=1527$) and 85% ($n=1531$) of mock-treated cells were clearly capable of membrane ruffling upon treatments with EGF and PDGF, respectively (Figure 6D and G). In contrast, Sra-1 suppression reduced the number of cells capable of this response to 27% (for EGF; $n=1049$) and 37% (for PDGF; $n=1287$) and Nap1 suppression to 12% (for EGF; $n=1409$) and 13% (for PDGF; $n=976$). Consequently, we conclude that both Sra-1 and Nap1 are essential for growth factor-induced membrane ruffling.

Loss of Sra-1 and Nap1 function precludes Rac-dependent actin reorganization

Abi proteins have been implicated in Rac activation by direct binding to and unmasking the Rac–GEF activity of SOS (Scita *et al*, 1999). As siRNA-mediated knockdown of Nap1, which

Figure 4 Interference with Sra-1 and Nap1 expression impairs lamellipodia formation in B16-F1 cells. (**A**) Time course of protein suppression upon siRNA expression. Samples from mock, Nap1 and Sra-1/PIR121 siRNA-treated B16-F1 cells were taken at days after transfection (tfx) as indicated and analysed for Nap1 or Sra-1 protein levels by Western blotting. Note the virtually complete suppression of Nap1 expression at days 3–5 and the significant reduction of Sra-1 at day 4 after transfection. (**B–C′**). Panels show the actin organization in representative B16-F1 cell populations treated with mock (B) and Nap1 siRNAs (C), respectively. (B′) and (C′) depict the cells quantified from (B) and (C), respectively. Only those cells that were mostly visible within the respective fields were counted and classified (B′, C′). Note the absence of lamellipodia in (C) as opposed to (B). Scale bar equals 20 μm. (**D**) Results of lamellipodia quantification. Values are means ± standard errors of means from three independent experiments. Cells were classified according to the categories (■) with or (□) without lamellipodia as well as (■) with ambiguous morphology. Note the correlation between Nap-1 and Sra-1 suppression (A) and reduction of the percentage of cells with lamellipodia (D). (**E**) Rac expression and activation by AlF is unchanged upon RNAi-mediated knockdown of Sra-1 and Nap1. Wild-type B16-F1 cells as well as mock, Sra-1 or Nap1 siRNA-treated cells express equal amounts of Rac (E, input). In addition, increased amounts of active Rac can be precipitated with PAK–PBD from all lysates upon AlF stimulation (E, PAK–PBD).

directly binds to Abi-1 (Yamamoto *et al*, 2001), impaired lamellipodia formation, we wondered whether signal transmission towards actin polymerization was blocked upstream or downstream of Rac activation. The observation that AlF treatment in B16-F1 cells induced Rac activation in both control and Nap1/Sra-1 knockdown populations, although the latter lacked lamellipodia, already suggested an essential function of these proteins downstream of Rac activation. To prove this assumption directly and to follow cell morphological changes upon Rac activation in mock versus Sra-1 and Nap1 knockdown cells in real time, we microinjected constitutively active L61Rac1 into VA-13 cells transiently (Figure 7; see also Figure 6A) or stably (not shown) expressing Sra-1- and Nap1-specific siRNAs.

In the first set of experiments, the actin cytoskeleton of at least 30 cells per experiment was analysed after microinjection of L61Rac1 followed by fixation and staining with phalloidin. In all, 88% of mock-treated cells ($n=91$) responded to L61Rac1 injection by forming prominent lamellipodia (Figure 7A). In contrast, 56% ($n=85$) of Sra-1 siRNA- and 73% ($n=89$) of Nap1 siRNA-treated cells were completely devoid of lamellipodial actin structures (for representative examples, see Figure 7B and C). The residual responsiveness of siRNA-treated cells to Rac1 injection was concluded to be due to incomplete suppression of gene expression, since counterstaining by indirect immunolabelling after microinjection confirmed the presence of the respective proteins in these subpopulations and their localization in lamellipodia (not shown), strengthening the correlation between the absence of either protein and lack of lamellipodia.

We then turned to single-cell analyses of Sra-1 and Nap1 knockdown populations, where we performed L61Rac1 injections during video microscopy using phase contrast optics. Representative frames from three out of more than 30 movies are shown in Figure 7D–F′. Cells lacking typical lamellipodia before injection were chosen for all experiments with siRNA-transfected as well as mock-transfected cells (Figure 7D–F). Mock-transfected cells responded immediately to L61Rac1 injection with lamellipodia formation around the entire cell periphery and maintained this morphology during video acquisition (at least 30 min) (Figure 7D and D′), while Sra-1 knockdown cells (Figure 7E and E′) and Nap1 knockdown cells (Figure 7F and F′) were incapable of forming lamellipodia upon Rac1 injection (see Supplementary movie 4). Together, these experiments demonstrate that Sra-1 and Nap1 are essential components of a signalling pathway driving actin rearrangements downstream of Rac activation.

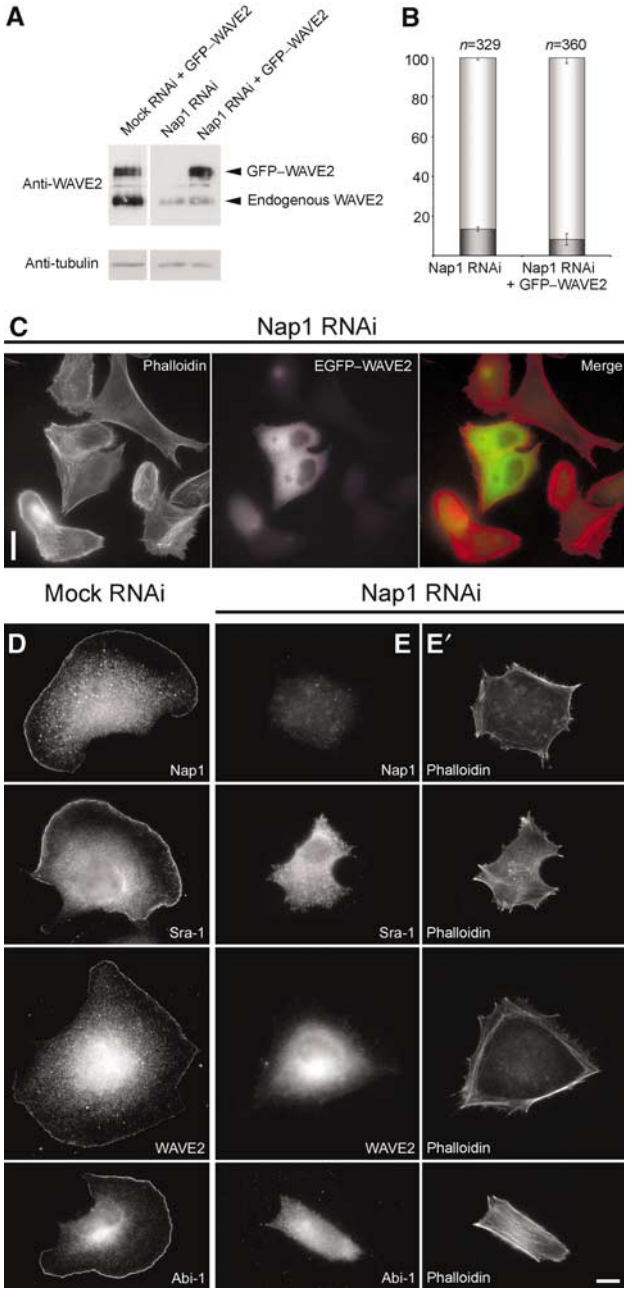

Discussion

It is well established that small GTPases of the Rho family are key regulatory switches in signalling pathways leading to reorganization of the actin cytoskeleton (Hall, 1998). In particular, Rac1 activation induces prominent actin structures at the cell periphery known as lamellipodia or

Figure 5 Lamellipodia formation is not restored by ectopic expression of WAVE2 in Nap1 ablated cells. Mock and Nap1 siRNA-treated B16-F1 cells with or without ectopic expression of GFP-tagged WAVE2 were analysed by Western blotting (**A**) or treated with AlF, fixed, stained and subjected to morphological analysis and quantification as described in Methods (**B**, **C**). Nap1 siRNA-treated cells expressing EGFP–WAVE2 were incapable of forming lamellipodia (C), although Western blotting confirmed successful expression of the GFP-tagged full-length WAVE2 protein (A). Note the significant reduction of expression of endogenous WAVE2 in Nap1 siRNA as compared to mock siRNA-treated cells (A). (B) Values are means ± standard errors of means from three independent experiments. Cells were classified according to the categories (■) with or (□) without lamellipodia. Note that ectopic expression of WAVE2 fails to increase the percentage of cells capable of lamellipodia formation (B). Measured differences between Nap1 knockdown populations with or without ectopic EGFP–WAVE expression were statistically not significant (paired *t*-test; $P=0.11$). (**D**–**E′**) Downregulation of Nap1 delocalizes Sra-1, WAVE2 and Abi-1. Mock (D) or Nap1 (E, E′) siRNA-treated B16-F1 cells were treated with AlF, fixed and stained with phalloidin (E′) or with antibodies as indicated (E). In contrast to mock-transfected controls (D), Sra-1, WAVE2 and Abi-1 were completely absent from peripheral actin structures of Nap1 siRNA-treated cells (E), which were unable to protrude lamellipodia (E′). Scale bars in (C) and (E′) equal 20 and 10 μm, respectively.

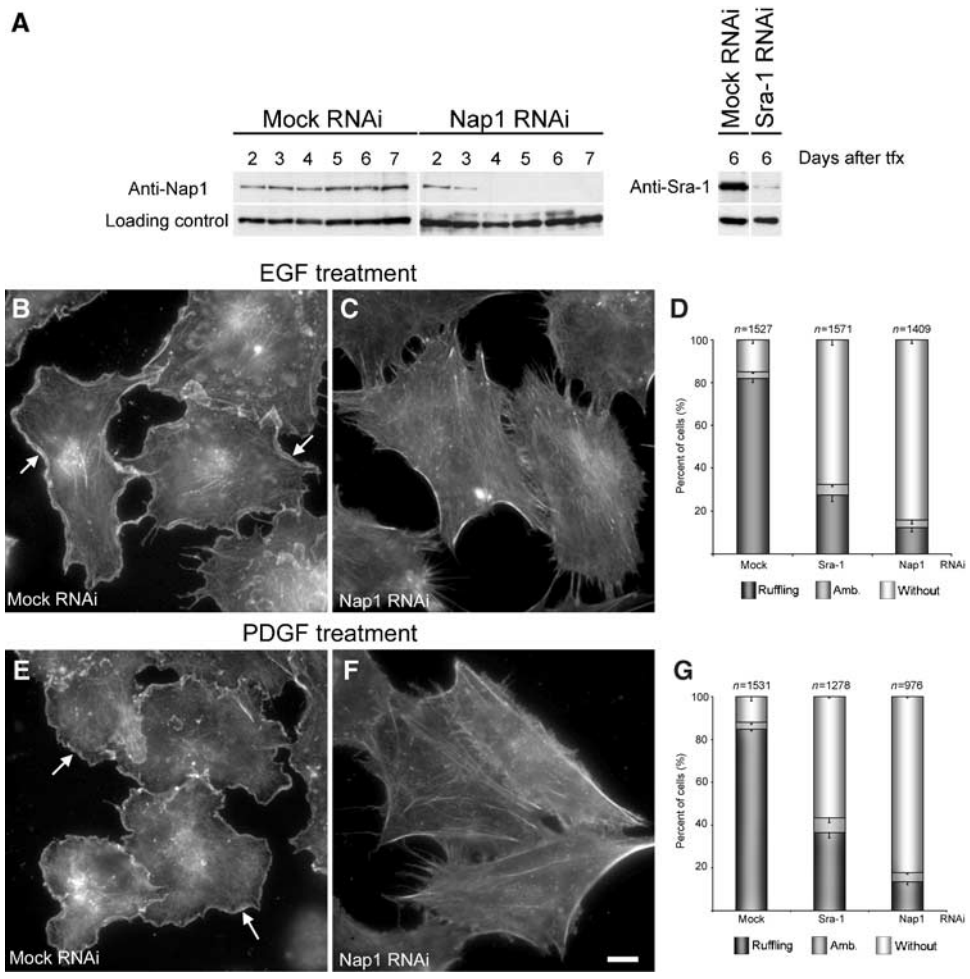

Figure 6 Interference with Sra-1 and Nap1 expression abolishes growth factor-induced membrane ruffling in VA-13 fibroblasts. (**A**) Evaluation of Nap1 and Sra-1 suppression upon siRNA expression. Samples from VA-13 cells transfected with mock, Nap1 and Sra-1 siRNA vectors were analysed by Western blotting at days 2–7 after transfection (tfx) as indicated. Note the absence of detectable levels of Nap1 expression beyond day 4 and the strong reduction of Sra-1 at day 6 after transfection. EGF and PDGF treatments shown in (**B–G**) were performed on day 6 after transfection. (B–G) Induction of membrane ruffling by EGF and PDGF. (B, C, E, F) Panels show the actin cytoskeleton of representative cell populations upon mock and Nap1 siRNA and growth factor treatments as indicated. Note the formation of lamellipodia and membrane ruffles (arrows in B, E) in mock-transfected controls induced by EGF and PDGF, respectively, and the absence of this response (C, F) after Nap1 knockdown. (D, G) Scale bar equals 10 μm. (D, G) Quantification of membrane ruffling upon EGF and PDGF treatments. Values are means ± standard errors of means from three independent counts. Cells were classified according to the categories (■) with or (□) without membrane ruffles as well as (■) with ambiguous morphology. Note the correlation between Nap-1 and Sra-1 suppression (A) and reduction of the percentage of cells capable of membrane ruffling upon growth factor treatments (D, G).

membrane ruffles (Ridley *et al*, 1992). Several Rac effector proteins capable of signalling to the actin cytoskeleton have been identified (Miki *et al*, 2000; Bokoch, 2003), but the exact sequence of events leading to the assembly of actin filaments driving lamellipodia protrusion is still not well understood. However, it is reasonable to assume that Arp2/3-based nucleation of actin filaments, catalysed by WAVE family proteins, is central to Rac-induced lamellipodia formation (Machesky and Insall, 1998; Miki *et al*, 1998). Elegant studies from *Drosophila* and *C. elegans* suggested that the orthologues of Sra-1/PIR121 and Nap1 act in a common signal transduction pathway linked to Rac-mediated cell migration (Hummel *et al*, 2000; Soto *et al*, 2002; Schenck *et al*, 2003). Interestingly, mammalian Nap1 and Sra-1 were reported to interact with Rac1 (Kitamura *et al*, 1997; Kobayashi *et al*, 1998) and more recently Nap1 and the isogene of Sra1, PIR121, with WAVE1 (Eden *et al*, 2002). *In vitro* experiments performed by the latter authors suggested that a complex of PIR121 and Nap1 acts inhibitory on WAVE1 function.

We have shown here that Sra-1 and Nap1 colocalize with Abi-1 and WAVE2 at the interface between the lamellipodial actin meshwork and the membrane. We have provided evidence that these proteins form stable complexes *in vivo* that can be immunoprecipitated from resting cells, upon Rac activation by AlF treatment and upon overexpression of constitutively active Rac. Furthermore, the four constituents of the complex are considerably pulled down by immobilized recombinant constitutively active Rac. We have also demonstrated that ablation of either protein, Sra-1 or Nap1, by RNAi causes severe alterations of the actin cytoskeleton, the most common feature of which is the disability to form lamellipodia and membrane ruffles. Experimental increase of activated Rac in knockdown cells, such as AlF treatment, growth factor stimulation or microinjection of constitutively active L61Rac did not restore lamellipodia formation in both Sra-1 and Nap1 siRNA-treated cells. In addition to Sra-1 and Nap1 protein ablation, these cells also displayed a significant reduction in WAVE2 expression levels as described earlier (Blagg *et al*,

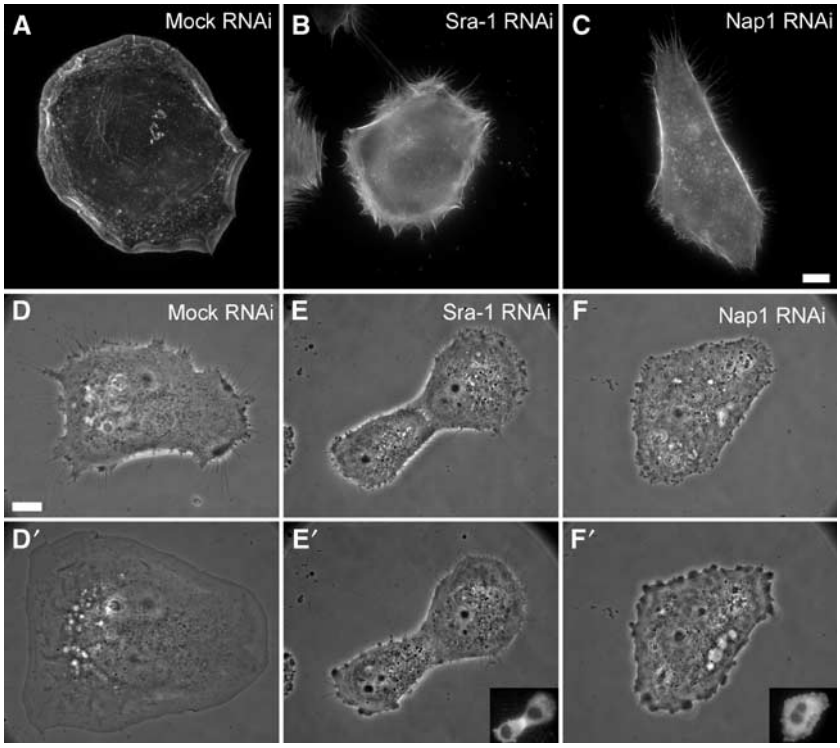

Figure 7 Loss of Sra-1 and Nap1 function abolishes Rac-dependent lamellipodia formation. (**A–C**) Organization of the actin cytoskeleton upon microinjection with L61Rac1. VA-13 fibroblasts treated as indicated were injected with L61Rac1, fixed and stained with fluorescent phalloidin. Sra-1 or Nap1 siRNA-treated cells (B, C) are completely devoid of lamellipodia upon injections as opposed to the control (A). (**D–F′**) Sra-1 and Nap1 siRNA-treated cells lack the ability to respond to Rac. The panels show video frames taken from representative examples 2 min before (D–F) or 30 min after injection (D′–F′). Within the 30 min time period after injection, the mock-treated cell has spread significantly (D, D′), while this response is absent in Sra-1 (E, E′) and Nap1 (F, F′) siRNA-treated cells. The success of Rac1 injections was monitored in all experiments by coinjection of fluorescent dextrane as exemplified by the insets in (E′, F′). Scale bar equals 5 μm.

2003; Rogers *et al*, 2003). However, we have also shown—by re-expressing EGFP–WAVE2—that the observed downregulation of endogenous WAVE2 in these cells is not causative of their disability to form lamellipodia.

From this we conclude that Sra-1 and Nap1 are essential constituents of a protein complex required for the formation of lamellipodia and ruffles. We therefore suggest that this protein complex, comprising at least four constituents (i.e. Sra-1, Nap1, Abi-1 and WAVE2), assembles with Arp2/3 to form the core of a multiprotein actin polymerase with catalytic and regulatory subunits that is targeted by Rac–GTP. Nevertheless, the exact mechanism of action of the holoenzyme driving lamellipodia protrusion requires in-depth future investigations.

However, our data support the view that the Sra-1/Nap1/Abi-1/WAVE2 complex exists in a preassembled form and that it is activated by an event (e.g. Rac activation) that also triggers its immediate recruitment to the cell periphery. Whether activation *in vivo*, which is expected to coincide with proper subcellular positioning, requires association with proteins additional to Rac or with nonproteinaceous components such as lipids remains to be established.

Mammalian fibroblasts and B16-F1 melanoma cells represent frequently used model systems to study motility and lamellipodia formation (Ballestrem *et al*, 1998). We have shown that the cell lines employed here lack detectable levels of WAVE1, the expression of which appears enriched in neuronal tissues (Sossey-Alaoui *et al*, 2003). As Nap1 and PIR121, the isogene of Sra-1, were reported to inhibit WAVE1-based actin nucleation *in vitro*, our findings, that is, that the same proteins are essential for membrane ruffling and lamellipodia formation in motile cells, appear somewhat surprising. Whether this discrepancy derives from potential differences of regulation between the three WAVE isoforms remains to be investigated, since cell biological experiments addressing the function of this complex in WAVE1-expressing model systems are lacking. Anyhow, our data pinpoint Sra-1 and Nap1 as essential intermediates of a signalling pathway from Rac activation to WAVE2-based nucleation of lamellipodial actin filaments.

From our studies, we cannot exclude that ADF/cofilin (Bokoch, 2003) downstream of Rac-dependent PAK activation or the interaction of active Rac1 with Irsp53 (Miki *et al*, 2000) are as relevant as Sra-1 and Nap1 for lamellipodia formation or membrane ruffling. However, our results entail that the former components are not sufficient for these processes in the absence of either Sra-1 or Nap1. Genetic inactivation or careful analysis upon RNAi targeting the multiple factors regulating membrane protrusion will help to define the exact sequence of events leading to the initiation and turnover of lamellipodial actin filaments.

Materials and methods

cDNA cloning and expression constructs

The murine Nap1 and Sra-1 cDNAs were obtained by reverse transcription–PCR on RNA from the brain of adult C57BL/6 mice, sequence verified and fused into pEGFP-C vectors (BD Biosciences,

Palo Alto, CA). EGFP–β actin, EGFP–WAVE2 and EYFP–Abi-1 have been described (Rietdorf *et al*, 2001; Stradal *et al*, 2001; Benesch *et al*, 2002).

Cells and transfections

B16-F1 mouse melanoma cells (ATCC CRL-6323) and VA-13 human lung fibroblasts (ATCC CCL-75.1) were grown in DMEM, 4.5 g/l glucose (Invitrogen, Germany) with 10% FCS (PAA Laboratories, Austria) and 2 mM glutamine at 37°C and 7% CO_2. NIH3T3 murine embryonic fibroblasts (ATCC CRL-1658) were maintained as above but with 10% FBS (Sigma, Germany). Swiss 3T3 fibroblasts (ATCC CCL-92) were grown in DMEM, 4.5 g/l glucose with 10% FBS (Sigma), 2 mM glutamine, 1 mM sodium pyruvate and 1% nonessential amino acids. Transfections were carried out with SuperFect (Quiagen, Germany, for B16-F1) or with FuGENE (Roche, Germany, for VA-13 and NIH 3T3), according to the manufacturers' protocols. Cells were plated on glass coverslips coated with 50 μg/ml fibronectin (Roche) or 25 μg/ml laminin (Sigma) prior to either fixation or video microscopy as indicated.

Immunofluorescence, video microscopy and microinjection

For immunolabellings, cells were fixed with 4% formaldehyde (PFA) in PBS for 3 min, extracted with a mixture of 0.1% Triton X-100 and PFA for 45 s followed by PFA for 15 min. For phalloidin stainings in Figures 4–7, cells were fixed with a mixture of 4% PFA and 0.25% glutaraldehyde in PBS for 20 min and extracted with 0.05% Triton X-100/PBS for 45 s. B16-F1 cells in Figures 1, 4B–E and 5 were treated with AlF as described (Hahne *et al*, 2001) 15 min prior to fixation. Alexa-dye-labelled secondary reagents and phalloidin were from Molecular Probes (The Netherlands). Video microscopy and microinjections were performed as described (Rottner *et al*, 1999a, b). L61Rac1 was purified as described (Ridley *et al*, 1992) and injected at 1.5 mg/ml in a mixture with 0.25 mg/ml Texas-Red-labelled dextrane (70 kDa, Molecular Probes).

Generation of antibodies

Polyclonal rabbit antisera termed Sra-1B, Nap1-A, Nap1-B and Nap1-C were raised against synthetic peptides derived from the murine sequences or for Sra-1A against a bacterially expressed GST-tagged fragment. For sequences, see Supplementary information. Anti-peptide antisera were affinity purified using the respective peptides immobilized on CNBr–sepharose 4B (Amersham Biosciences, Sweden). The specificity of the antisera was confirmed by Western blot detection of the endogenous and ectopically expressed GFP-tagged antigens. The sequence from peptide Sra-1B is identical to the corresponding sequence in the PIR121 isogene, ensuring the recognition of Sra-1 and PIR121. Generation of the monoclonal anti-Abi-1 antibody and the polyclonal anti-pan-WAVE antiserum will be described elsewhere (Innocenti *et al*, 2004).

Immunoprecipitations and pulldown assays

For immunoprecipitations, B16-F1 cells grown in 10 cm diameter dishes were washed with PBS and lysed in 500 μl of ice-cold lysis buffer L1 (12 mM Tris base, 8 mM HEPES, 50 mM NaCl, 15 mM KCl, 1.5 mM $MgCl_2$, 1 mM EGTA, 10 mM $Na_2H_2P_2O_7$, 1 mM ATP, 20 mM NaF, 1 mM Na_3VO_4, 1% PEG 8000, 1% Triton X-100 and Complete Mini^{TM}, EDTA-free protease inhibitor (Roche)) for 20 min on ice. Cleared lysates were incubated with anti-Nap1 or anti-Sra-1 antibodies for 1 h and followed by incubation with protein G–sepharose beads (Amersham Biosciences) for 45 min at 4°C on a rotary wheel. Beads were then washed twice with lysis buffer without NaF, Na_3VO_4, ATP and Triton X-100. Precipitates were resolved by SDS–PAGE and analysed by immunoblotting. Immunoprecipitations shown in Figure 2D were performed using lysis buffer L1 containing 10 mM $MgCl_2$ and lacking $Na_2H_2P_2O_7$ and ATP. Monoclonal anti-Rac antibodies were from Upstate Biotechnology (Lake Placid).

For Rac activation assays, GST fusion of PAK–PBD (residues 65–136 of PAK3; kindly provided by G Bokoch, The Scripps Research Institute, La Jolla) was immobilized on glutathione–sepharose (Amersham Biosciences) in buffer A (50 mM Tris, pH 7.5, 50 mM NaCl, 15 mM $MgCl_2$, Complete Mini^{TM}). Cell lysates from B16-F1 cells were prepared as follows: dishes with 1×10^7 B16-F1 cells were treated with either DMEM or DMEM containing 30 mM NaF and 50 μM $AlCl_3$ for 15 min and then lysed with 500 μl of ice-cold lysis buffer (25 mM Tris, pH 7.5, 10 mM $MgCl_2$, 150 mM NaCl, 1% Igepal, 5% sucrose, Complete Mini^{TM}). Activated Rac–GTP was precipitated from whole-cell lysates with 20 μl glutathione–sepharose beads coupled with GST–PBD. For pulldown assays with recombinant Rac, GST–L61Rac and GST as control were immobilized on glutathione–sepharose beads in buffer B (50 mM Tris, pH 7.5, 50 mM NaCl, 5 mM $MgCl_2$, 0.1 mM DTT). For pulldowns, B16-F1 cells grown to confluence in 10 cm diameter dishes were washed with PBS supplemented with 5 mM $MgCl_2$ and lysed in 500 μl lysis buffer L1 containing 15 mM $MgCl_2$ and lacking $Na_2H_2P_2O_7$ and ATP. In all, 30 μl of 2.5 mg/ml GST–L61Rac or GST alone coupled to glutathione–sepharose beads were incubated with the cell lysates for 1 h at 4°C. Samples were analysed as described for immunoprecipitations.

RNA interference

Following the published method (Brummelkamp *et al*, 2002), oligonucleotides harbouring the respective 19-nt target sequences were ligated into the pSUPER.retro.puro vector (OligoEngine, Seattle, WA). Vectors were verified by sequencing. For full oligonucleotide and targeting sequences, see Supplementary information. Cells were transfected overnight with the respective vectors and then replated into selection medium containing puromycin to eliminate nontransfected cells. The maximum efficiency of gene product suppression was assessed by Western blotting as described below. In addition to Sra-1, B16-F1 cells were found to express low amounts of PIR121. Hence, for Sra-1/PIR121 knockdown experiments in these cells, cotransfections with both Sra-1- and PIR121-specific knockdown vectors were performed in all experiments. Mock transfections were performed with pSUPER.retro.puro followed by puromycin selection identical to the experiments with knockdown vectors.

Quantification of lamellipodia in B16-F1 cells

Cells were transfected with vectors silencing either Nap1 or Sra-1 and PIR121 expression or with control pSUPER.retro.puro. At 16–20 h after transfection, cells were replated onto fibronectin-coated coverslips and selected for 72 h with puromycin (2.5 μg/ml), treated with AlF for 15 min, fixed and stained for filamentous actin with phalloidin. More than 550 cells from three independent experiments were photographed and analysed for each condition. For Western blotting, aliquots of transfected cells were plated in dishes with selection medium and a sample was taken every 24 h for 4 days. Anti-α-tubulin monoclonal antibody YL1/2 (Wehland *et al*, 1983) was routinely used as a loading control.

For ectopic expression of GFP-tagged WAVE2 in Figure 5, control and knockdown cell populations were treated as above, except that cells were transfected with EGFP–WAVE2 16 h prior to analysis. In all, 360 EGFP–WAVE2-expressing cells from three independent experiments were subjected to morphological analysis and quantification. Besides immunofluorescence, cell populations prepared in parallel were assayed for successful expression of the GFP-tagged construct. Statistical analyses were carried out using SigmaPlot8.0 (SPSS Inc., Chicago, IL) and Minitab 10.5 software (Minitab Inc., State College). Quantification details are given in the Supplementary information.

Analyses of membrane ruffling and lamellipodia formation in VA-13 fibroblasts

Cells were transfected with vectors silencing either Sra-1 or Nap1 expression or with control pSUPER.retro.puro and replated into selection medium with puromycin (1 μg/ml) the next day. For experiments upon transient interference with gene expression, cells were plated onto fibronectin-coated coverslips and between days 5 and 7 after transfections subjected to growth factor treatments or video microscopy and microinjection. For quantifications of growth factor-induced ruffling, cells on coverslips were serum starved for 30 min in DMEM and then stimulated for 15 min in DMEM containing 100 ng/ml EGF (human recombinant EGF, Sigma) or 10 ng/ml PDGF (human recombinant PDGF BB, Sigma). For each condition, at least 900 cells were analysed and quantified (for details, see table in Supplementary information). For analyses of actin cytoskeletal organization shown in Figure 7A–C, 30–60 cells were microinjected within a time period of 15 min, incubated for an additional 15 min, fixed and stained with phalloidin. For Western blotting, aliquots of transfected cells were plated in dishes with selection medium and a sample was taken every 24 h for 6 days. For

the generation of stable cell lines, aliquots of transfected cells were serially diluted in selection medium and approximately 200 clones were isolated and expanded. All clones were tested by Western blotting and clones displaying the highest degree of gene product reduction were subjected to subcloning.

Accession numbers

The cDNA sequences of murine Nap1 and Sra-1 have been deposited in the EMBL Nucleotide Sequence Database under accession numbers AJ534525 and AJ567911, respectively.

Supplementary data

Supplementary data are available at *The EMBO Journal* Online.

Acknowledgements

We are grateful to Roger Y Tsien for kindly providing mRFP cDNA. We thank Petra Hagendorff for excellent technical assistance. This work was supported in part by the DFG (STR 666/1-1 to TEBS and JW and STR 666/2-1 to TEBS and KR) and the DAAD (Vigoni program to JW).

References

Ballestrem C, Wehrle-Haller B, Imhof BA (1998) Actin dynamics in living mammalian cells. *J Cell Sci* **111** (Part 12)**:** 1649–1658

Benard V, Bokoch GM (2002) Assay of Cdc42, Rac, and Rho GTPase activation by affinity methods. *Methods Enzymol* **345:** 349–359

Benesch S, Lommel S, Steffen A, Stradal TE, Scaplehorn N, Way M, Wehland J, Rottner K (2002) Phosphatidylinositol 4,5-biphosphate (PIP2)-induced vesicle movement depends on N-WASP and involves Nck, WIP, and Grb2. *J Biol Chem* **277:** 37771–37776

Biesova Z, Piccoli C, Wong WT (1997) Isolation and characterization of e3B1, an eps8 binding protein that regulates cell growth. *Oncogene* **14:** 233–241

Blagg SL, Stewart M, Sambles C, Insall RH (2003) PIR121 regulates pseudopod dynamics and SCAR activity in Dictyostelium. *Curr Biol* **13:** 1480–1487

Bokoch GM (2003) Biology of the p21-activated kinases. *Annu Rev Biochem*

Brummelkamp TR, Bernards R, Agami R (2002) A system for stable expression of short interfering RNAs in mammalian cells. *Science* **296:** 550–553

Campbell RE, Tour O, Palmer AE, Steinbach PA, Baird GS, Zacharias DA, Tsien RY (2002) A monomeric red fluorescent protein. *Proc Natl Acad Sci USA* **99:** 7877–7882

Eden S, Rohatgi R, Podtelejnikov AV, Mann M, Kirschner MW (2002) Mechanism of regulation of WAVE1-induced actin nucleation by Rac1 and Nck. *Nature* **418:** 790–793

Geese M, Schluter K, Rothkegel M, Jockusch BM, Wehland J, Sechi AS (2000) Accumulation of profilin II at the surface of Listeria is concomitant with the onset of motility and correlates with bacterial speed. *J Cell Sci* **113** (Part 8)**:** 1415–1426

Geijsen N, van Delft S, Raaijmakers JA, Lammers JW, Collard JG, Koenderman L, Coffer PJ (1999) Regulation of p21rac activation in human neutrophils. *Blood* **94:** 1121–1130

Hahne P, Sechi A, Benesch S, Small JV (2001) Scar/WAVE is localised at the tips of protruding lamellipodia in living cells. *FEBS Lett* **492:** 215–220

Hall A (1998) Rho GTPases and the actin cytoskeleton. *Science* **279:** 509–514

Hummel T, Leifker K, Klambt C (2000) The *Drosophila* HEM-2/NAP1 homolog KETTE controls axonal pathfinding and cytoskeletal organization. *Genes Dev* **14:** 863–873

Innocenti M, Zucconi A, Disanza A, Frittoli E, Areces L, Steffen A, Stradal TEB, Di Fiore PP, Carlier MF, Scita G (2004) Abi1 is essential for the formation and activation of a WAVE2 signaling complex mediating Rac-dependent actin remodeling. *Nat Cell Biol* (in press)

Kitamura T, Kitamura Y, Yonezawa K, Totty NF, Gout I, Hara K, Waterfield MD, Sakaue M, Ogawa W, Kasuga M (1996) Molecular cloning of p125Nap1, a protein that associates with an SH3 domain of Nck. *Biochem Biophys Res Commun* **219:** 509–514

Kitamura Y, Kitamura T, Sakaue H, Maeda T, Ueno H, Nishio S, Ohno S, Osada S, Sakaue M, Ogawa W, Kasuga M (1997) Interaction of Nck-associated protein 1 with activated GTP-binding protein Rac. *Biochem J* **322** (Part 3)**:** 873–878

Kobayashi K, Kuroda S, Fukata M, Nakamura T, Nagase T, Nomura N, Matsuura Y, Yoshida-Kubomura N, Iwamatsu A, Kaibuchi K (1998) p140Sra-1 (specifically Rac1-associated protein) is a novel specific target for Rac1 small GTPase. *J Biol Chem* **273:** 291–295

Machesky LM, Insall RH (1998) Scar1 and the related Wiskott–Aldrich syndrome protein, WASP, regulate the actin cytoskeleton through the Arp2/3 complex. *Curr Biol* **8:** 1347–1356

Miki H, Suetsugu S, Takenawa T (1998) WAVE, a novel WASP-family protein involved in actin reorganization induced by Rac. *EMBO J* **17:** 6932–6941

Miki H, Yamaguchi H, Suetsugu S, Takenawa T (2000) IRSp53 is an essential intermediate between Rac and WAVE in the regulation of membrane ruffling. *Nature* **408:** 732–735

Nakagawa H, Miki H, Nozumi M, Takenawa T, Miyamoto S, Wehland J, Small JV (2003) IRSp53 is colocalised with WAVE2 at the tips of protruding lamellipodia and filopodia independently of Mena. *J Cell Sci* **116:** 2577–2583

Nozumi M, Nakagawa H, Miki H, Takenawa T, Miyamoto S (2003) Differential localization of WAVE isoforms in filopodia and lamellipodia of the neuronal growth cone. *J Cell Sci* **116:** 239–246

Ridley AJ (1998) Mammalian cell microinjection assay to study the function of Rac and Rho. *Methods Mol Biol* **84:** 153–160

Ridley AJ (2001) Rho family proteins: coordinating cell responses. *Trends Cell Biol* **11:** 471–477

Ridley AJ, Paterson HF, Johnston CL, Diekmann D, Hall A (1992) The small GTP-binding protein rac regulates growth factor-induced membrane ruffling. *Cell* **70:** 401–410

Rietdorf J, Ploubidou A, Reckmann I, Holmstrom A, Frischknecht F, Zettl M, Zimmermann T, Way M (2001) Kinesin-dependent movement on microtubules precedes actin-based motility of vaccinia virus. *Nat Cell Biol* **3:** 992–1000

Rogers SL, Wiedemann U, Stuurman N, Vale RD (2003) Molecular requirements for actin-based lamella formation in *Drosophila* S2 cells. *J Cell Biol* **162:** 1079–1088

Rottner K, Behrendt B, Small JV, Wehland J (1999a) VASP dynamics during lamellipodia protrusion. *Nat Cell Biol* **1:** 321–322

Rottner K, Hall A, Small JV (1999b) Interplay between Rac and Rho in the control of substrate contact dynamics. *Curr Biol* **9:** 640–648

Schenck A, Bardoni B, Langmann C, Harden N, Mandel JL, Giangrande A (2003) CYFIP/Sra-1 controls neuronal connectivity in *Drosophila* and links the Rac1 GTPase pathway to the fragile X protein. *Neuron* **38:** 887–898

Scita G, Nordstrom J, Carbone R, Tenca P, Giardina G, Gutkind S, Bjarnegard M, Betsholtz C, Di Fiore PP (1999) EPS8 and E3B1 transduce signals from Ras to Rac. *Nature* **401:** 290–293

Sossey-Alaoui K, Head K, Nowak N, Cowell JK (2003) Genomic organization and expression profile of the human and mouse WAVE gene family. *Mamm Genome* **14:** 314–322

Soto MC, Qadota H, Kasuya K, Inoue M, Tsuboi D, Mello CC, Kaibuchi K (2002) The GEX-2 and GEX-3 proteins are required for tissue morphogenesis and cell migrations in *C. elegans*. *Genes Dev* **16:** 620–632

Stradal T, Courtney KD, Rottner K, Hahne P, Small JV, Pendergast AM (2001) The Abl interactor proteins localize to sites of actin polymerization at the tips of lamellipodia and filopodia. *Curr Biol* **11:** 891–895

Wehland J, Willingham MC, Sandoval IV (1983) A rat monoclonal antibody reacting specifically with the tyrosylated form of alpha-tubulin. I. Biochemical characterization, effects on microtubule polymerization *in vitro*, and microtubule polymerization and organization *in vivo*. *J Cell Biol* **97:** 1467–1475

Witke W, Podtelejnikov AV, Di Nardo A, Sutherland JD, Gurniak CB, Dotti C, Mann M (1998) In mouse brain profilin I and profilin II

associate with regulators of the endocytic pathway and actin assembly. *EMBO J* **17:** 967–976

Yamamoto A, Suzuki T, Sakaki Y (2001) Isolation of hNap1BP which interacts with human Nap1 (NCKAP1) whose expression is down-regulated in Alzheimer's disease. *Gene* **271:** 159–169

Yamazaki D, Suetsugu S, Miki H, Kataoka Y, Nishikawa S, Fujiwara T, Yoshida N, Takenawa T (2003) WAVE2 is required for directed cell migration and cardiovascular development. *Nature* **424:** 452–456

Yan C, Martinez-Quiles N, Eden S, Shibata T, Takeshima F, Shinkura R, Fujiwara Y, Bronson R, Snapper SB, Kirschner MW, Geha R, Rosen FS, Alt FW (2003) WAVE2 deficiency reveals distinct roles in embryogenesis and Rac-mediated actin-based motility. *EMBO J* **22:** 3602–3612